IFSCC 2025 full paper (IFSCC-1127)

Silica Capsule with UV and Blue Light Protection

Wonjun Jang [1] , Hyuck Lim [1] , Eun Hee Choi [1] , Yeonggi Kim [1] and Kyounghee Shin [1,*]

[1] R&D center, SUNJIN BEAUTY SCIENCE, Seoul, Korea, South

1. Introduction

The increasing reliance on digital devices and artificial light sources has significantly elevated human exposure to blue light, also known as high-energy visible (HEV) light, with wavelengths ranging from 400 to 500 nm. While blue light is naturally present in sunlight, its artificial sources, such as LED screens and fluorescent lighting, have intensified its impact on human health, particularly skin health. Unlike ultraviolet (UV) rays, which are well-documented for their harmful effects, blue light penetrates deeper into the skin, reaching the dermis where collagen and elastin reside. This deep penetration generates reactive oxygen species (ROS), leading to oxidative stress, DNA damage, and the degradation of essential skin proteins like collagen and elastin. Over time, these processes contribute to premature aging, hyperpigmentation, and compromised skin barrier function [1-4]. The growing body of evidence underscores the urgent need for effective strategies to mitigate the detrimental effects of blue light on the skin.

The growing awareness of the adverse effects associated with organic UV filters, such as skin absorption risks and marine ecosystem disruption [5], has driven a shift toward encapsulated alternatives. Organic filters like avobenzone, while effective against UVA radiation, face criticism for systemic absorption linked to endocrine disruption concerns and photodegradation into toxic byproducts that harm coral reefs [6]. To mitigate these issues, encapsulation technologies—including cellulose, lipid, polymer, and silica-based systems—have emerged as promising solutions [7-9]. Among these, silica capsules stand out due to their ability to stabilize UV filters, prevent direct skin contact, and reduce environmental leaching. Studies demonstrate that silica encapsulation enhances avobenzone's photostability while minimizing cutaneous uptake and marine toxicity. Additionally, silica's inert nature and compatibility with mineral filters like zinc oxide enable synergistic broad-spectrum UV protection without compromising cosmetic appeal. These advantages position silica capsules as a transformative approach to reconciling efficacy, safety, and environmental sustainability in modern sunscreen formulations [10,11].

In this study, we present a novel solution: colored silica capsules designed to block both UV and blue light while ensuring skin compatibility and stability. By chelating avobenzone (AB) with transition metals, these silica capsules exhibit a shifted absorption spectrum that effectively attenuates blue light transmission. Compared to conventional formulations, these capsules demonstrate superior efficacy in reducing blue light exposure while maintaining excellent photostability and cosmetic acceptability. This innovation not only addresses the limitations of traditional sunscreens but also minimizes the risks associated with organic UV

filters by encapsulating them within a silica matrix. The development of such advanced materials represents a significant step forward in creating safer and more effective skincare formulations tailored for modern environmental challenges.

2. Materials and Methods

1. Material

Butyl methoxydibenzoylmethane (Avobenzone, AB) was supplied from DSM, Porous spherical silica (SUNJIN BEAUTY SCIENCE, Korea) were used. Tetraethylorthosilicate (TEOS) was purchased from Evonik Industries (Germany). Iron standard solution was purchased from Kanto Chemical (Singapore).

2. Preparation of Silica Capsules with UV and HEV protection

The AB was melted and loaded into porous silica particles under precise temperature and shear force control to prevent crystallization. A thin silica layer was coated onto the AB-loaded particles to prevent leakage, using a water-soluble silica precursor at controlled pH and temperature. Finally, the outer layer was chelated with Fe^{3+} ions, and the AB-loaded silica capsules were filtered and dried to obtain the final samples.

3. Characterization

The surface area and pore volume of porous silica, AB-loaded silica capsule (SiO_2-AB), zinc ion-AB chelated silica capsule (SiO_2-BLP) were measured using the Brunauer-Emmett and Teller technique (BET). Nitrogen adsorption desorption isotherms were measured using a Micromeritics Tristar II 3020 surface area and porosity analyzer. After AB loading, the samples were analyzed by high-performance liquid chromatography (HPLC) for AB quantification. UV-visible absorbance spectra were obtained to confirm the formation of the AB-Fe chelation on the surface of the silica capsules (Lambda 1050, PerkinElmer, Inc., CT, USA).

4. Water Dispersibility and Redispersity Test

The dispersion behavior of 1 g of AB-loaded silica powder was evaluated by dispersing it in 40 g of distilled water at 25°C with stirring. After 1 day, the redispersibility was assessed by inverting the dispersion container.

5. Leakage Test of AB from Silica Capules

The leakage of AB from AB-loaded silica capsules was evaluated by dispersing 10 g of the powder in 20 g of 2,3-butylene glycol at 25°C, followed by stirring at 1000 rpm for 5 minutes. After 1 day, AB leakage into the solvent was assessed by observing AB crystals on black paper treated with the mixture and by optical microscopy and polarized light microscopy.

6. Whiteness Test

The whiteness of SiO2-AB and SiO_2-BLP was compared by applying them to the skin in powder form. TiO_2 powder was also tested in the same manner.

7. Sun Protection Factor and UVA Protection Factor Analyses

Using AB, SiO_2-AB (30% AB), and SiO_2-BLP (30% AB) as a UV blocking raw material, a series of sunscreens were formulated as shown in Table 1. First, phase A was prepared by thoroughly dispersing the polymer in water. Phase B was then heated to approximately 80°C to fully dissolve the UV filter and emulsifier. Once both phases A and B reached a temperature of 75–80°C, phase B was added to phase A, and the mixture was emulsified at 5,000 rpm for 5

minutes. The emulsion was then cooled to 45°C, followed by the addition of phase C, which was thoroughly dispersed.The resulting sunscreen formulations were evaluated for their UV protection performance through in vitro measurements. The Solar Light SPF-290AS (Solar Light, USA) was used to measure SPF and PA values. For the test, each sample was applied to a PMMA plate (Solar Light, USA) at a thickness of 0.75 mg/cm² and dried for 15 minutes. The sun protection factor was measured using the SPF-290AS device after four minimal erythema dose (MED) pre-irradiations. The final SPF and PA values were calculated as the average of measurements taken at nine locations on the PMMA plate.

Table 1. Formulation recipe for in vitro SPF and UVA test

Phase	INCI Name	#1	#2	#3
A	Water	49.95	49.95	49.95
	Polyacrylate Crosspolymer-6	0.25	0.25	0.25
	Hydroxyethyl Acrylate/Sodium Acryloyldimethyl Taurate Copolymer	0.20	0.20	0.20
B	Cetearyl Olivate, Sorbitan Olivate	1.20	1.20	1.20
	Bis-Ethylhexyloxyphenol Methoxyphenyl Triazine	2.00	2.00	2.00
	Octocrylene	2.00	2.00	2.00
	Ethylhexyl Salicylate	5.00	5.00	5.00
	Ethylhexyl Methoxycinnamate	3.50	3.50	3.50
	Isoamyl p-Methoxycinnamate	4.00	4.00	4.00
	Butyl Methoxydibenzoylmethane (AB)	3.00	-	-
	Diethylamino hydroxybenzoyl hexyl benzoate	-	-	-
	Ethylhexyl triazone	-	-	-
	Glyceryl Stearate, PEG-100 Stearate	0.90	0.90	0.90
	Glyceryl Stearate	0.90	0.90	0.90
	Polysorbate 60	1.50	1.50	1.50
C	Water	10.00	10.00	10.00
	Silica, Butyl Methoxydibenzoylmethane (SiO_2-AB)	**-**	10.00	-
	Silica, Butyl Methoxydibenzoylmethane (SiO_2-BLP)	**-**	-	10.00
	Silica	**7.00**		-
	Propanediol	5.00	5.00	5.00
	Butylene glycol	2.00	2.00	2.00
	1,2-Hexanediol	1.50	1.50	1.50
	Ethylhexylglycerin	0.10	0.10	0.10

8. Stability Test

To evaluated the stability of AB and AB-Fe chelation, the series of sunscreen formulations were stored at 60°C and monitored for color change.

3. Results

Avobenzone, a widely used UVA filter, faces limitations such as photodegradation, skin permeation risks, sticky texture upon application, and recrystallization during storage, which compromise its efficacy and safety. To address these challenges, we engineered a silica-based encapsulation strategy. By immobilizing avobenzone within a porous silica matrix (SiO_2-AB), we aimed to (1) mitigate skin irritation by preventing direct contact with the compound, (2) improve sensory properties by reducing tackiness, and (3) inhibit recrystallization to maintain uniform UV protection over time. Furthermore, we incorporated Fe^{3+}-mediated chelation to modulate the composite's optical properties, enabling dual UV and blue light (400–500 nm) blocking capabilities. This approach leverages Fe^{3+}'s coordination chemistry with avobenzone's functional groups (e.g., carbonyl and enol moieties), which not only stabilizes the UV filter against photodegradation but also extends absorption into the blue light spectrum (SiO_2-BLP). By forming a Fe^{3+}-avobenzone complex at the outmost silica matrix, the composite achieves tunable light-filtering characteristics while maintaining silica's inherent advantages (Figure 1).

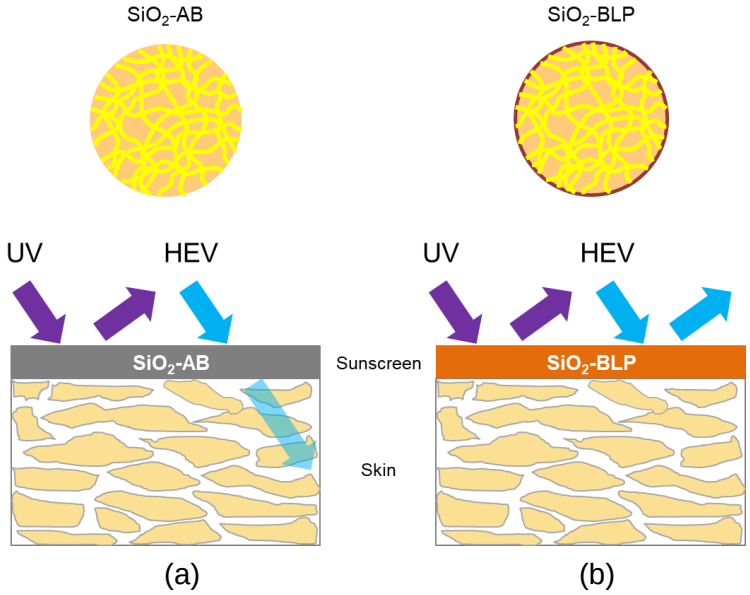

Figure 1. Schematic illustration of silica capsules with UV and blue light protection: (a) SiO_2-AB: Avobenzone-immobilized within a porous silica matrix, (b) SiO_2-BLP: Additional Fe^{3+}-mediated chelation on the SiO_2-AB.

The observed changes in BET surface area values (Table 2) after loading 30% of avobenzone onto silica and subsequent chelation with Fe^{3+} ions provide clear evidence of successful avobenzone immobilization. The pristine silica exhibited a high BET surface area, characteristic of its porous structure. Upon avobenzone loading, a significant reduction in surface area occurred, indicating that avobenzone molecules occupied the silica's pores and surface sites, effectively reducing the available adsorption area. Further changes in BET values after Fe^{3+} chelation suggest structural reorganization: the Fe ions likely formed coordination bonds with avobenzone's carbonyl and enolic groups, creating a more compact composite. The sequential BET variations—initial decrease post-loading and subsequent modulation after Fe treatment—collectively confirm that avobenzone was successfully anchored to the silica support, with Fe^{3+} chelation further stabilizing the system. These results align with the expected physicochemical behavior of hybrid silica-drug composites, where surface area reduction is a hallmark of effective guest-molecule incorporation [12].

Table 2. BET surface area at different synthesis stages of SiO_2-BLP

Sample	BET value (m^2/g)	BJH pore volume (cm^3/g)	Average pore size (nm)
Porus silica	108.6102	0.550145	13.7072
SiO_2-AB	1.6700	0.069967	26.3528
SiO_2-BLP	1.2859	0.036138	28.9764

To evaluate the light-blocking performance of the synthesized composites, UV/Vis/NIR spectroscopy was employed to analyze the absorption spectra of SiO_2-AB (avobenzone-loaded silica) and SiO_2-BLP (Fe^{3+}-chelated avobenzone-silica). The SiO_2-AB particles exhibited strong absorption exclusively in the UVA range (320–400 nm), consistent with avobenzone's intrinsic photoproperties. In contrast, the SiO_2-BLP particles demonstrated a broadened absorption profile of 450-550 nm, extending into HEV blue light region. This spectral shift confirms successful chelation between Fe^{3+} and avobenzone within the silica matrix, as the metal-ligand coordination modifies the electronic transitions of avobenzone, enabling HEV protection. The retention of UVA absorption in both systems further validates effective avobenzone loading, as unencapsulated avobenzone would typically degrade or leach out during processing. These results align with the encapsulation strategy's dual objectives: maintaining UV filtering efficacy while adding blue light protection—a critical feature for modern sunscreen formulations targeting digital screen-induced skin damage.

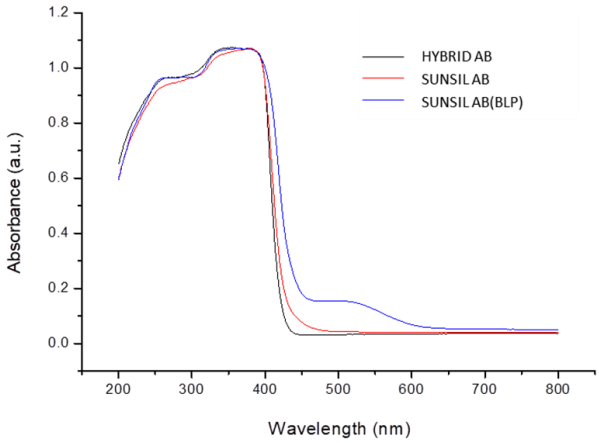

Figure 2. UV/Vis/NIR absorption spectra of silica capsules.

To evaluate the colloidal water-dispersibility, the silica capsules were dispersed in water, followed by a 1-day sedimentation and redispersion test. As shown in Figure 3, both SiO_2-AB and SiO_2-BLP particles exhibited excellent aqueous dispersibility. Furthermore, after 1 day, settled particles were easily redispersed into a uniform suspension with mild shaking, leaving no residual aggregates at the container base. This behavior confirms effective surface passivation by the silica matrix, which minimizes interparticle van der Waals forces and prevents irreversible agglomeration. The lack of permanent sedimentation further indicates that avobenzone remains encapsulated within the silica framework without surface leakage, as free avobenzone would typically promote hydrophobicity-driven clumping. These results under-

score the dual role of silica encapsulation: enhancing compatibility with aqueous formulations while maintaining physicochemical stability under storage conditions.

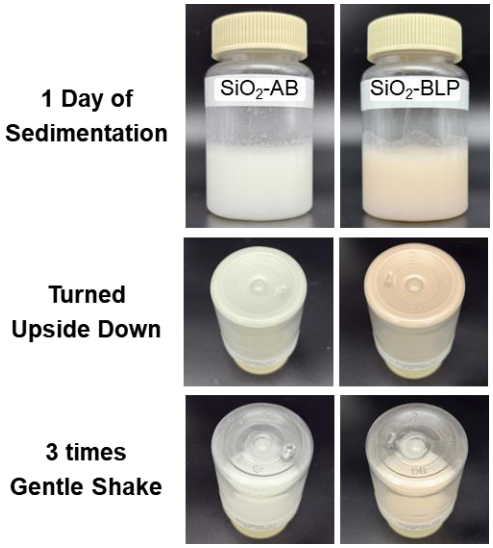

Figure 3. Water dispersibility and redispersity test of silica capsules.

The leakage assessment revealed no visible crystals on black paper or detectable birefringence signals under polarized microscopy, confirming the absence of AB release from silica capsules (Figure 4). This absence of phase-separated AB crystals demonstrates the silica matrix's ability to fully encapsulate and retain the UV filter, even in glycol-based solvents commonly used in cosmetic formulations. The results correlate with the reduced BET surface area and stable optical properties observed earlier, collectively verifying that the silica encapsulation effectively prevents recrystallization and maintains formulation integrity under storage conditions.

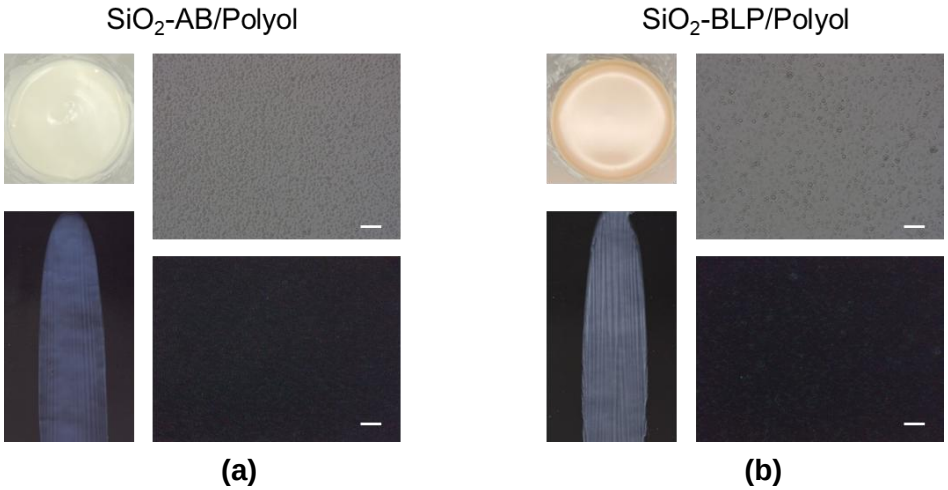

Figure 4. Visual and microscopic analysis of avobenzone leakage from silica capsules in polyol (2,3-butylene glycol): Observations of appearance, black paper tests, optical microscopy images, and polarized light microscopy images of (a) SiO_2-AB dispersion and (b) SiO_2-BLP dispersion. Scale bar is 30 μm.

The silica encapsulation of AB not only stabilizes AB within the porous silica matrix but also resolves the aesthetic drawbacks of inorganic sunscreens, aligning with consumer demand for cosmetically elegant formulations. Due to silica's low refractive index (~1.46), the SiO_2-AB particles exhibited minimal white cast (Figure 5a), maintaining skin transparency unlike titanium dioxide (refractive index ~2.7) or zinc oxide (~2.0) (Figure 5c). This transparency is critical for cosmetically elegant sunscreen formulations. For SiO_2-BLP particles, a notable color shift to brown (Figure 5b) further reduced residual whitening. The brown hue, arising from Fe^{3+}-avobenzone charge-transfer complexes, closely matched natural skin tones, effectively masking the white cast associated with unmodified silica or metal oxides. This dual mechanism—inherent low refractive index and skin-tone-mimicking coloration—demonstrates the system's superiority in balancing UV protection with aesthetic appeal.

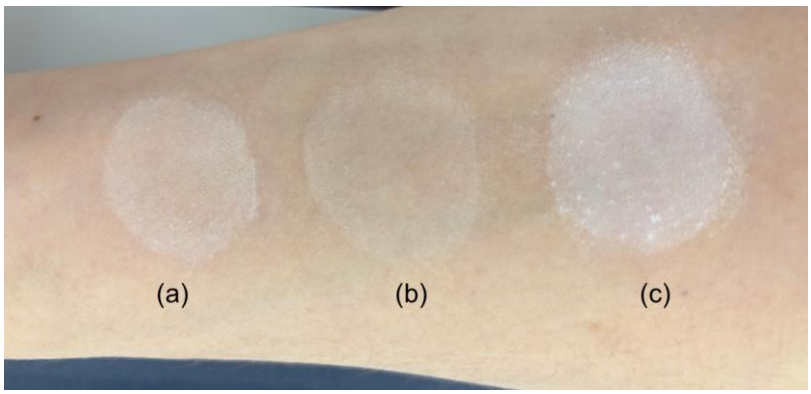

Figure 5. White cast test images of (a) SiO_2-AB (b) SiO_2-BLP, and (c) TiO_2 powders.

The *in vitro* SPF and PA evaluations revealed significant improvements in UV protection for silica-encapsulated avobenzone systems compared to free avobenzone. The unencapsulated AB formulation exhibited modest performance with an SPF of 11.8 and PA of 6.7, while the SiO_2-AB (30% avobenzone) and SiO_2-BLP (30% avobenzone) systems demonstrated enhanced efficacy, achieving SPF 22.52/PA 12.55 and SPF 21.3/PA 11.9, respectively. The comparable performance between SiO_2-AB and SiO_2-BLP suggests that silica encapsulation itself—rather than Fe^{3+} chelation—plays the dominant role in stabilizing avobenzone and optimizing its dispersion within the sunscreen matrix. Surprisingly, the Fe^{3+}-mediated chelation in SiO_2-BLP introduced HEV blocking capabilities without compromising UV protection efficiency. This indicates that the coordination between Fe^{3+} and AB's functional groups broadens the absorption spectrum while preserving the UV-filtering activity of AB. The absence of a trade-off between HEV protection and UV efficacy highlights a key advantage of this hybrid system: it achieves multifunctional broad-spectrum protection without sacrificing performance in either domain. The results align with the optical absorption data, where SiO_2-BLP exhibited extended absorption into the 450–550 nm range, demonstrating that the structural and electronic modifications from chelation synergistically enhance light-blocking versatility. The 2-fold increase in SPF for encapsulated systems aligns with silica's ability to prevent avobenzone aggregation, ensuring uniform film formation on the PMMA plate and maximizing UV-filtering efficiency. The higher PA values further indicate improved UVA protection, likely due to reduced photodegradation of AB when confined within the silica framework. These results underscore silica encapsulation as a critical strategy for enhancing both UVB and UVA protection in sunscreen formulations.

Table 3. UV protection performance of silica-encapsulated avobenzone formulations

Sample	Details	*In vitro* SPF	*In vitro* PA
#1	Free avobenzone	11.80	6.70
#2	SiO_2-AB	22.52	12.55
#3	SiO_2-BLP	21.30	11.90

In addition, the accelerated stability testing under high-temperature conditions (60°C, 3 months) revealed no detectable discoloration or degradation in the SiO_2 -BLP formulation, confirming robust thermal stability. This resistance to color change contrasts with conventional avobenzone formulations, which often exhibit yellowish discoloration due to photodegradation byproducts or recrystallization. The observed stability arises from two synergistic mechanisms: (1) the silica matrix physically confines avobenzone, preventing molecular aggregation or oxidative degradation pathways, and (2) Fe^{3+}-avobenzone coordination strengthens the composite's structural integrity, suppressing thermally induced charge-transfer variations that could alter optical properties. These results validate SiO_2 -BLP's suitability for long-term storage in diverse climatic conditions while maintaining its skin-tone-matching brown hue—a critical advantage for commercial sunscreen products requiring consistent aesthetic quality.

Figure 6. Color stability of the SiO_2-BLP formulation under prolonged high-temperature storage.

4. Discussion

The silica-based encapsulation of avobenzone (SiO_2-AB) and its Fe^{3+}-chelated derivative (SiO_2-BLP) effectively addressed key limitations of conventional avobenzone formulations. The observed reduction in BET surface area after avobenzone loading confirmed successful immobilization within the silica matrix, minimizing direct skin contact and mitigating irritation risks. Fe^{3+} chelation further stabilized the composite via coordination with avobenzone's carbonyl/enol groups, as evidenced by structural reorganization in BET analysis and extended absorption into the blue light spectrum (450–550 nm). This dual UV/HEV protection aligns with modern demands for broad-spectrum sunscreens, particularly given rising concerns about digital screen-induced skin damage. The absence of avobenzone recrystallization and excellent aqueous redispersibility underscore silica's role in enhancing formulation stability and compatibility with cosmetic bases—critical for long-term storage and user compliance. Notably, the 2-fold increase in SPF/PA values for encapsulated systems (SPF 22.52 vs. 11.8) highlights

silica's ability to optimize avobenzone dispersion and prevent photodegradation, though Fe^{3+} chelation primarily contributed to HEV protection without compromising UV efficacy. Aesthetic improvements, such as reduced white cast (refractive index ~1.46) and skin-tone-matching brown hues from Fe^{3+}-AB complexes (Figure 5), address a longstanding consumer barrier to mineral sunscreen adoption. However, the study's in vitro focus warrants future in vivo tests to assess cutaneous permeation and real-world photostability under diverse environmental conditions.

5. Conclusion

This study demonstrates that silica encapsulation synergizes with Fe^{3+} chelation to transform avobenzone into a multifunctional photoprotective agent. By resolving avobenzone's inherent instability, sensory drawbacks, and limited spectrum, the SiO_2-BLP system achieves dual UV/HEV protection, enhanced SPF/PA efficacy, and improved cosmetic elegance. The strategy not only advances sunscreen technology but also provides a template for stabilizing hydrophobic actives in other dermatological formulations. Future research should explore scalability for industrial production and long-term safety profiles in human trials.

6. Acknowledgements

This research was supported by the Technological Innovation R&D Program (RS-2023-00277456) funded by the Ministry of SMEs and Startups (MSS, Korea).

7. References

[1] Orawan S.., Cheng Y., Yanyun M., Wei Liu, *Skin Pharmacol. Physiol.* 2022;35, 305–318.
[2] Kim, M., Kim, H., Lee, Y. H., Kim, J. E., *Photochem. Photobiol.*, 2022, 98(3), 680–688.
[3] Jeong, S. Y., Kim, H. N., Jung, H. D., Lee, W. J., Park, Y. M., *Biomolecules*, 2020, 10(12), 1610.
[4] Talib, J., Albroaih, H., Din, F. U., Alqahtani, A., Alqahtani, M. S., Jameel, *J.Antioxidants*, 2021, 10(6), 899.
[5] National Academies of Sciences, Engineering, and Medicine. *Review of Fate, Exposure, and Effects of Sunscreens in Aquatic Environments and Implications for Sunscreen Usage and Human Health*; The National Academies Press: Washington, DC, 2022.
[6] Ana J., Emília S., Maria T. C., Honorina C., José M. Sousa L., Isabel F. A., *Pharmaceuticals* 2022, 15, 263.
[7] Gasparro M. P., Mitchnick M., Nash J., *Adv. Drug Deliv. Rev.*, 2011, 473-482.
[8] Pooja G. B., Shubham S. S., GSC Biol. Pharm. Sci., 2024, 28(2), 199–207.
[9] Wang W. H., Liang H. T., Yang-Wang Y. T., Shih C. J., *RSC Advances*, 2020, 27, 15846–15852.
[10] Green L.J., Bhatia N. D., Toledano O., Erlich M., Spizuoco A., Goodyear B.C., York J.P., Jakus J., *Arch. Dermatol. Res.,* 2023, 315, 2787–2793.
[11] Ma Q., Zhang Y., Huangfu Y., Gao S., Zhou C., Rong H., Deng L., Dong A., Zhang J., *ACS Appl. Mater. Interfaces* 2023, 15(9), 12209–12220.
[12] Charnay, C.; Bégu, S.; Tourné-Péteilh, C.; Nicole, L.; Lerner, D.A.; Devoisselle, J.M. *Eur. J. Pharm. Biopharm.* 2004, 58 (3), 743–748.